

Photonic chirped radio-frequency generator with ultra-fast sweeping rate and ultra-wide sweeping range

Jhhih-Min Wun,¹ Chia-Chien Wei,² Jyehong Chen,³ Chee Seong Goh,⁴ S. Y. Set,⁴
and Jin-Wei Shi^{1*}

¹Department of Electrical Engineering, National Central University, Zhongli, 320, Taiwan

²Department of Photonics, National Sun Yat-sen University, Kaohsiung, 804, Taiwan

³Department of Photonics, National Chiao Tung University, Hsinchu 300, Taiwan

⁴Alnair Labs Corporation, Tokyo, Japan

*jwshi@ee.ncu.edu.tw

Abstract: A high-performance photonic sweeping-frequency (chirped) radio-frequency (RF) generator has been demonstrated. By use of a novel wavelength sweeping distributed-feedback (DFB) laser, which is operated based on the linewidth enhancement effect, a fixed wavelength narrow-linewidth DFB laser, and a wideband (dc to 50 GHz) photodiode module for the hetero-dyne beating RF signal generation, a very clear chirped RF waveform can be captured by a fast real-time scope. A very-high frequency sweeping rate (10.3 GHz/ μ s) with an ultra-wide RF frequency sweeping range (\sim 40 GHz) have been demonstrated. The high-repeatability (\sim 97%) in sweeping frequency has been verified by analyzing tens of repetitive chirped waveforms.

©2013 Optical Society of America

OCIS codes: (060.5625) Radio frequency photonics; (140.2020) Diode lasers.

References and links

1. A. G. Stove, "Linear FMCW radar techniques," *IEE Proc. F* **139**, 343–350 (1993).
2. K. B. Cooper, R. J. Dengler, N. Llombart, T. Bryllert, G. Chattopadhyay, E. Schlecht, J. Gill, C. Lee, A. Skalare, I. Mehdi, and P. H. Siegel, "Penetrating 3-D imaging at 4- and 25-m range using a submillimeter-wave radar," *IEEE Trans. Microw. Theory Tech.* **56**(12), 2771–2778 (2008).
3. A. Y. Nashashibi, K. Sarabandi, P. Frantzis, R. D. De Roo, and F. T. Ulaby, "An ultrafast wide-band millimeter wave (MMW) polarimetric radar for remote sensing applications," *IEEE Trans. Geosci. Rem. Sens.* **40**(8), 1777–1786 (2002).
4. Z. D. Taylor, R. S. Singh, D. B. Bennett, P. Tewari, C. P. Kealey, N. Bajwa, M. O. Culjat, A. Stojadinovic, H. Lee, J.-P. Hubschman, E. R. Brown, and W. S. Grundfest, "THz medical imaging: in vivo hydration sensing," *IEEE Trans. Terahertz Sci. Technol.* **1**(1), 201–219 (2011).
5. C. S. Ruf and J. Li, "A correlated noise calibration standard for interferometric, polarimetric, and autocorrelation microwave radiometers," *IEEE Trans. Geosci. Rem. Sens.* **41**(10), 2187–2196 (2003).
6. T. Nagatsuma, T. Kumashiro, Y. Fujimoto, K. Taniguchi, K. Ajito, N. Nukutsu, T. Furuta, A. Wakatsuki, and Y. Kado, "Millimeter-wave imaging using photonics-based noise source," *Proc. IRMMW-THz 2009*, 34th International Conference on Infrared, Millimeter, and Terahertz Waves, Busan, South Korea, Sept., 1–2 (2009).
7. R. J. Trew, "Design theory for broad-band YIG-tuned FET oscillators," *IEEE Trans. Microw. Theory Tech.* **27**(1), 8–14 (1979).
8. Y.-W. Huang, T.-F. Tseng, C.-C. Kuo, Y.-J. Hwang, and C.-K. Sun, "Fiber-based swept-source terahertz radar," *Opt. Lett.* **35**(9), 1344–1346 (2010).
9. K. B. Cooper, R. J. Dengler, N. Llombart, T. Bryllert, G. Chattopadhyay, I. Mehdi, and P. H. Siegel, "An approach for sub-second imaging of concealed objects using terahertz (THz) radar," *J Infrared Milli Terahz Waves* **30**, 1297–1307 (2009).
10. K. B. Cooper, R. J. Dengler, N. Llombart, A. Talukder, A. V. Panangadan, C. S. Peay, I. Mehdi, and P. H. Siegel, "Fast, high resolution terahertz radar imaging at 25 meters," *Proc. SPIE* **7671**, 76710Y-1 - 76710Y-8 (2010).
11. J. D. McKinney, D. E. Leaird, and A. M. Weiner, "Millimeter-wave arbitrary waveform generation with a direct space-to-time pulse shaper," *Opt. Lett.* **27**(15), 1345–1347 (2002).
12. M. Li and J. P. Yao, "Photonic generation of continuously tunable chirped microwave waveforms based on a temporal interferometer incorporating an optically-pumped linearly-chirped fiber Bragg grating," *IEEE Trans. Microw. Theory Tech.* **59**(12), 3531–3537 (2011).

13. R. E. Saperstein, N. Alić, D. Panasenکو, R. Rokitski, and Y. Fainman, "Time-domain waveform processing by chromatic dispersion for temporal shaping of optical pulses," *J. Opt. Soc. Am. B* **22**(11), 2427–2436 (2005).
14. J.-W. Lin, C.-L. Lu, H.-P. Chuang, F.-M. Kuo, J.-W. Shi, C.-B. Huang, and C.-L. Pan, "Photonic generation and detection of W-band chirped millimeter-wave pulses for radar," *IEEE Photon. Technol. Lett.* **24**(16), 1437–1439 (2012).
15. J.-W. Shi, F.-M. Kuo, N.-W. Chen, S. Y. Set, C.-B. Huang, and J. E. Bowers, "Photonic generation and wireless transmission of linearly/nonlinearly continuously tunable chirped millimeter-wave waveforms with high time-bandwidth product at W-band," *IEEE J. Photonics* **4**(1), 215–223 (2012).
16. B. R. Biedermann, W. Wieser, C. M. Eigenwillig, T. Klein, and R. Huber, "Direct measurement of the instantaneous linewidth of rapidly wavelength-swept lasers," *Opt. Lett.* **35**(22), 3733–3735 (2010).
17. Y. Zhou, K. K. Y. Cheung, Q. Li, S. Yang, P. C. Chui, and K. K. Y. Wong, "Fast and wide tuning wavelength-swept source based on dispersion-tuned fiber optical parametric oscillator," *Opt. Lett.* **35**(14), 2427–2429 (2010).
18. J.-W. Shi, F.-M. Kuo, T. Chiueh, H.-F. Teng, H. J. Tsai, N.-W. Chen, and M.-L. Wu, "Photonic generation of millimeter-wave white-light at W-Band using a very-broad-band and high-power photonic emitter," *IEEE Photon. Technol. Lett.* **22**, 847–849 (2010).
19. Z.-F. Fan and M. Dagenais, "Optical generation of a megahertz-linewidth microwave signal using semiconductor lasers and a discriminator-aided phase-locked loop," *IEEE Trans. Microw. Theory Tech.* **45**(8), 1296–1300 (1997).
20. S. Ristic, A. Bhardwaj, M. J. Rodwell, L. A. Coldren, and L. A. Johansson, "An optical phase-locked loop photonic integrated circuit," *J. Lightwave Technol.* **28**(4), 526–538 (2010).
21. O. C. Graydon, M. N. Zervas, and R. I. Laming, "Erbium-doped-fiber optical limiting amplifiers," *J. Lightwave Technol.* **13**(5), 732–739 (1995).
22. A. Villafranca, J. A. Lázaro, I. Salinas, and I. Garcés, "Measurement of the linewidth enhancement factor in DFB lasers using a high-resolution optical spectrum analyzer," *IEEE Photon. Technol. Lett.* **17**(11), 2268–2270 (2005).
23. K. Shi, R. Watts, D. Reid, T. N. Huynh, C. Browning, P. M. Anandarajah, F. Smyth, and L. P. Barry, "Dynamic linewidth measurement method via an optical quadrature front end," *IEEE Photon. Technol. Lett.* **23**(21), 1591–1593 (2011).

1. Introduction

The generation of sweeping (chirped) radio-frequency (RF) to sub-THz waveforms with a broad frequency sweeping range has attracted a lot of attention due to their usefulness for a variety of applications, such as in high-resolution frequency modulated continuous wave (FMCW) or chirped pulses radar [1–3], bio-medical imaging systems [4], and for the characterization of wide-band devices/circuits or radio telescopes [5]. Compared with using the MMW white-light (noise) source to acquire the high-resolution radar imaging [6], using the chirped RF source can offer a much faster frame rate of imaging. One of the major types of MMW (RF) sweeping-frequency (chirped) source is the scanning yttrium iron garnet (YIG) oscillator [7]. However, the YIG oscillator usually needs a high-output voltage (tens of volts) driving circuit and exhibits a usual frequency scanning rate of around 1GHz/ms [8], which is usually too low to obtain a real-time image with very-high frame rate. By combining the frequency-sweeping (1.6-3.2 GHz) direct digital signal synthesizer (DDS) with the chain of sub-MMW frequency multipliers and MMW power amplifier [9], sub-THz (~660 GHz) chirped waveform generation with fast ramp rate (59 MHz/μs), a wide bandwidth (~30 GHz) [2,9], and a large pulse compression ratio, have been demonstrated. By use of such wide-bandwidth (~30 GHz) sub-THz chirped waveform, a high resolution (< 1 cm range resolution) radar image has also been demonstrated [10].

In order to further break the limitation on scanning rate and bandwidth, an attractive alternative is to use photonic techniques to generate a MMW (RF) chirped waveform [11–14]. In most of the reported photonic microwave chirped pulse generation schemes, the working principle is mainly based on the direct frequency-to-time mapping technique [11–14]. Such technique is enabled by sending a short optical pulse through a long single-mode fiber so the accumulated quadratic spectral phase impresses a large linear chirp onto the resulting time-domain waveform. In a very recent work, chirped MMW pulses with a high central frequency of 40 GHz and a wide scanning range (10 to 55 GHz) has been experimentally demonstrated with pulse durations around 1.2 ns [12]. However, in these reported complex pulse shaper systems, a truly continuous chirp waveform with a large tunability in terms of generated (linear/nonlinear) waveform, compression ratio (time-bandwidth product), center frequency,

and sweeping rate, is very difficult to achieve due to the limited frequency resolution of pulse shaper system or fiber Bragg grating (FBG).

In this paper, a novel simple scheme for photonic generation of chirped RF (or sub-THz) signal is proposed. Through the use of a special designed 1.55 μm distributed feedback (DFB) laser module with a narrow instantaneous linewidth during wavelength sweeping, a wideband photodiode module (dc to 50 GHz), and the heterodyne-beating technique, we experimentally demonstrate the truly continuous chirped RF signal with ultra-high ramp rate (10.3 GHz/ μs), wide scanning bandwidth (~ 40 GHz), and an extremely high time-bandwidth product (compression ratio). The high-repeatability ($\sim 97\%$) in sweeping frequency has been verified by analyzing tens of repetitive chirped RF waveforms. By use of such proposed system, the sub-THz chirped waveform can be simply obtained by adjusting the wavelength difference between the sweeping and fixed-wavelength lasers and using a photodiode with a sub-THz optical-to-electrical (O-E) bandwidth [14,15].

2. Measurement setup and sweeping laser

Figure 1 shows the schematic of our experimental setup. The optical MMW signal is simply generated by the hetero-dyne beating technique. A wavelength sweeping laser is used for the generation of fast-sweeping MMW chirped waveform. Compared with the typical reported frequency sweeping lasers, our laser has the unique advantage to provide a narrow (< 10 MHz) instantaneous linewidth during wavelength sweeping, which is a key issue to generate the chirped waveform. Although most of the reported sweeping lasers [16,17] exhibit a narrow static linewidth with a much larger wavelength sweeping range, they may have a very-poor dynamic linewidth ($> \text{GHz}$) during wavelength sweeping. This would result in the wideband MMW white-noise spectra during heterodyne-beating signal generation with optical wavelength sweeping [18]. Thanks to the narrow instantaneous linewidth of our sweeping laser, a clear and repeatable instantaneous MMW waveform can be displayed on the very-fast real-time scope, as discussed latter. This result indicates the reasonable good phase noise of our photo-generated MMW signal. In order to further reduce the phase noise in our proposed scheme, an optical phase-locked loop (OPLL) [19,20] with ultra-fast response time may be preferred [20] to dynamic locking the phase between two lasers during fast wavelength-sweeping.

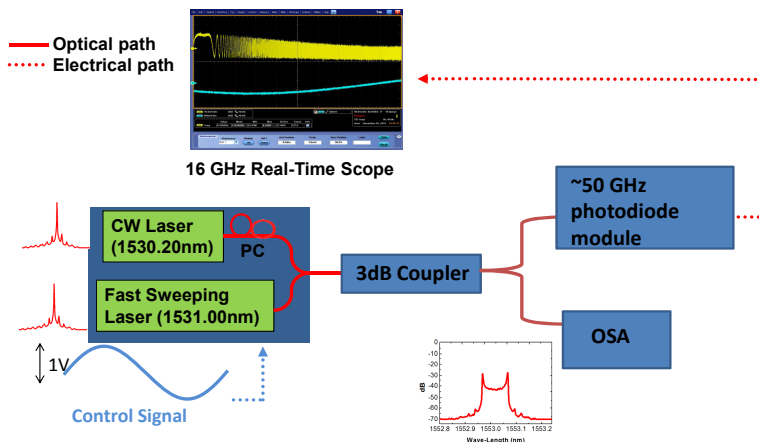


Fig. 1. The experimental setup for chirped pulse generation. OSA: optical spectrum analyzer

The conceptual diagram of function blocks of our fast wavelength-swept laser source is given in our previous work. It is mainly composed of a commercial available distributed feedback (DFB) laser chip (NEL Laser Diodes NLK5C5EBKA), alternating current (AC) laser current driving circuit, and an optical limiting amplifier [21]. Compared with the sweeping laser reported in our previous work [15], the central wavelength is shifted from

1530 to 1550 nm, which is more convenient for the use of high-power erbium doped fiber amplifier (EDFA) to obtain the strong optical beating signal. During wavelength sweeping operation, the driving circuit is used to convert and amplify the external injected voltage signal into current waveforms to effectively modulate the output optical amplitude of DFB laser. Due to the existence of linewidth enhancement factor (chirp parameter) in DFB laser [22], the values of central wavelength would also be swept with the variation of output optical power (injected carrier density). In order to obtain strong linewidth enhancement effect (frequency modulation; FM), huge amplitude of current pulses (hundreds of mA) is necessary to modulate our DFB laser chip. However, this should definitely accompany the significant output amplitude modulation (AM), which is not desired for our application. An optical limiting amplifier is thus integrated with the output of DFB laser chip to minimize serious power fluctuation during wavelength sweeping. Figures 2(a), 2(b), and 2(c) shows the output optical spectrum of our sweeping laser measured under different sweeping rates (and driving voltages) at 10 KHz, 100 KHz and 1 MHz, respectively. The central wavelength of sweeping laser under static operation (no AC driving signal injection) is also shown here for reference. As can be seen, the scanning wavelength range would definitely enhance with the increase of amplitude of driving voltage. Nevertheless, when the sweeping rate reaches 1 MHz, as shown in Fig. 2(c), the wavelength sweeping range becomes narrowing. Such degradation in scanning bandwidth can be mainly attributed to the limited 3-dB bandwidth (around 1.0 MHz) of current driving circuit in our sweeping laser system.

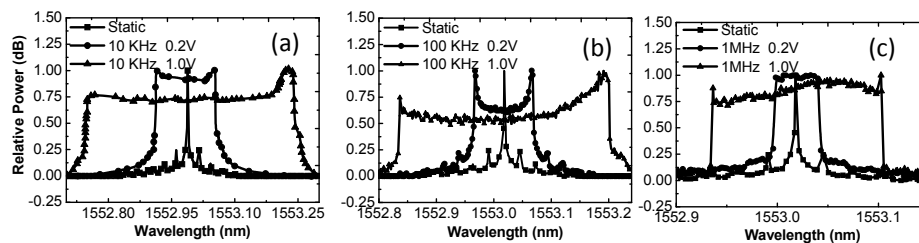


Fig. 2. The measured optical spectra of our fast sweeping laser under different sweeping rates at 10 KHz (a), 100 KHz (b), and 1 MHz (c) with different driving voltages (0.2 and 1 V).

Figure 3 shows the measured scanning bandwidth versus peak-to-peak driving voltage (V_{pp}) under different sweeping rates. We can clearly see that at 1 KHz sweeping rate and 0.9 V_{pp} driving, the maximum scanning bandwidth of our sweeping laser can attain 70 GHz. On the other hand, when the sweeping rate reaches 1 MHz, the bandwidth significantly decreases to around ~20 GHz. Under the highest modulation speed we tested (up to 3 MHz), the scanning bandwidth becomes zero. There is thus a significant trade-off between sweeping rate and scanning bandwidth in our laser system. Compared with the wavelength sweeping laser reported in our previous work [15], our new laser system can achieve a much wider scanning bandwidth (~40 vs. ~14 GHz) and with a much faster scanning rate (100 vs. 10 KHz). As shown in Fig. 1, by combining such sweeping signal with the output from a fixed-wavelength laser, we can obtain a heterodyne-beating signal with a time-varying beating frequency. If the linearly chirped pulse waveform is desired, which means that the beating frequency varies linearly with time, we can inject the triangle waveform into the sweeping laser and let the separation of two beating optical wavelengths linearly varies with time [15]. On the other hand, if the nonlinearly chirped pulse is preferred, it can be simply generated by using a sinusoidal signal as the control signal of sweeping laser. Overall, by use of this proposed scheme, a truly continuous chirped waveform with excellent tunability, which includes chirped rate, waveform, and central frequency, can be easily realized by changing the waveform and the frequency of AC driving signal of laser.

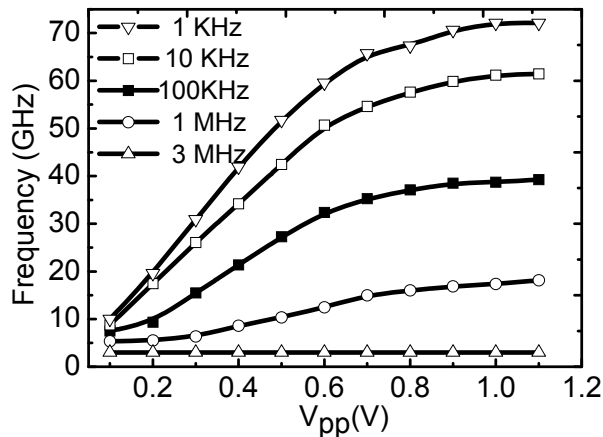


Fig. 3. The measured frequency sweeping range of our laser under different sweeping rate (1 KHz, 10 KHz, 100 KHz, 1 MHz, and 3 MHz) and different driving voltage (V_{pp})

3. Measurement results and analysis

After combing the chirped laser signal with another fix-wavelength co-polarized CW laser light, as shown in Fig. 1, the combined signal is detected by a photodiode module with a near 50 GHz bandwidth (Anritsu; MN4765A) and captured by an oscilloscope (Tektronix® DPO71254) with sample rate of 50 GS/s. A total number of 10,000,000 samples are recorded each time during single measurement. Figure 4 shows the typical waveform captured at near dc frequency. During such measurement, the AC voltage driving signal is sinusoidal signal with 1 V_{pp} and 100 KHz frequency. As can be seen, a significant chirp waveform can be observed.

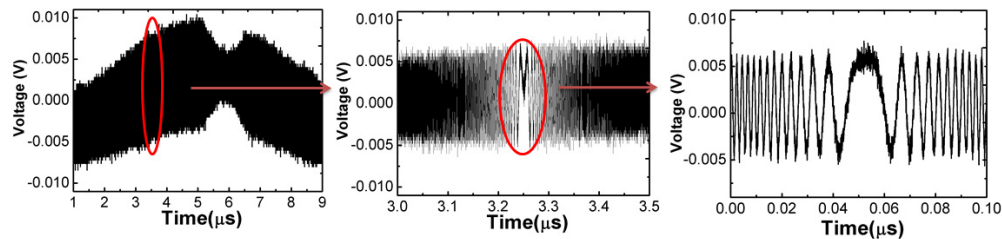


Fig. 4. The captured chirped waveform at near dc frequency

The maximum measurement bandwidth of our real-time scope is at around 16 GHz and Fig. 5 shows the captured waveform at the time near (over) the edge of maximum measurement bandwidth (~ 16 GHz). We can clearly see that when the sweeping frequency is over 16 GHz, a significant decrease in the measured amplitude would happen and the captured waveforms become unreliable.

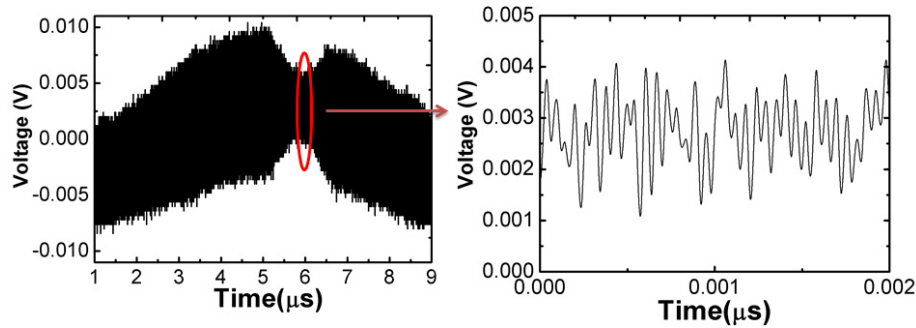


Fig. 5. The captured chirped waveform at the frequency over the maximum bandwidth of real-time scope (16 GHz)

The dynamic frequency difference between two lasers (instantaneous sweeping frequency) can be estimated by applying a very-short gating window to the captured signal, and the frequency difference within each block is assumed to be constant. Then, employing discrete Fourier transform (DFT) to a block of the gated signal, the corresponding instantaneous frequency would be estimated as the peak frequency of the calculated spectrum. In order to increase the frequency resolution of the estimation, which is the reciprocal of the time length of the signal, the number of samples used in DFT is increased by assembling the blocks gated at the same position of each period, as shown by Fig. 6 [23]. The calculated results are exhibited in Fig. 7. These waveforms are all measured by use of AC sinusoidal voltage driving signal with $1 V_{pp}$.

Due to the 16 GHz bandwidth of the oscilloscope, the estimated frequency of over 16 GHz is distorted and unreliable, as discussed in Fig. 5, and it is not plotted in Fig. 7. The sweeping rates of Figs. 7(a) and 7(b) are 100 KHz and 10 KHz, and therefore, the maximum repeated times of the captured waveforms (under maximum sampling rate: 50 GS/s) are 20 and 2, respectively. This is limited by the size of memory installed in our real-time scope. For the case in Fig. 7(a), the gated sample numbers of each block is set as 16 in our calculation, and the corresponding frequency resolution is 156 MHz. Similarly, the frequency resolution of the other case shown in Fig. 7(b) is set the same, so that its sample numbers of each block is 160. As shown in Fig. 7, we can clearly see that compared with laser under 100 KHz sweeping rate, the measured sweeping frequency shows a less fluctuation under a lower sweeping rate (10 KHz). This phenomenon implies that a higher sweeping rate would induce a poorer dynamic linewidth during wavelength sweeping and this should definitely degrade the quality or generated chirp waveform. The laser action requires strong material gain as well as enough build-up time to achieve a stable lasing condition with narrow linewidth. When a laser is swept across wavelength with time, these conditions would be compromised and the dynamic linewidth should be further broadened with the increase of sweeping rate due to the fact that the coherent time of instantaneous wavelength becomes shorter and shorter. The maximum frequency sweeping rates can be estimated by the slope of traces in Fig. 7 and their numbers are about 10.3 and 1.4 GHz/ μ s under 100 and 10 KHz driving, respectively. Consequently, based on the estimated sweeping rate, the maximum frequency shifts within each time block will be 3.3 MHz and 4.5 MHz, which are much smaller than the frequency resolution (156 MHz) in our calculation. This truth confirms the feasibility of assuming constant frequency in each time block during our calculation. Moreover, the repeatability of wavelength sweeping is also examined by frequency correlation between repeated signals captured in different time. Without taking the frequency of over 16 GHz into consideration, the correlation coefficients between the frequencies of signals captured in different time slots are up to 97% and 99% for the cases of 100 KHz and 10 KHz sweeping rates, respectively. Accordingly, the repeatability of sweeping frequency is very high.

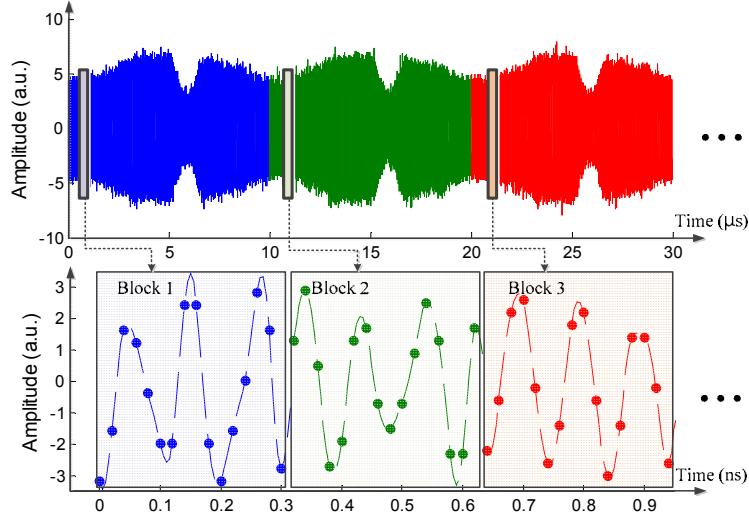


Fig. 6. The schematic plot of dynamic frequency measurement

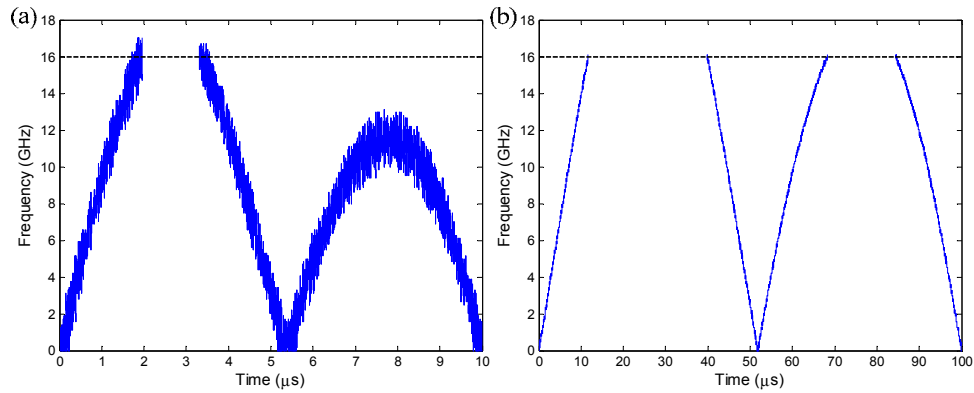


Fig. 7. The estimated instantaneous frequency with the sweeping rates of (a) 100 KHz and (b) 10 KHz

4. Conclusion

In conclusion, we have demonstrated a novel photonic RF chirped pulse generation system. It is mainly composed of a novel wavelength sweeping laser, which is driven by the linewidth enhancement effect, and the heterodyne-beating setup. By use of such proposed system, ultrafast ramp rate (10.3 GHz/ μ s), wide scanning bandwidth (\sim 40 GHz), and high repeatability in the sweeping frequency (\sim 97%) have been successfully demonstrated. Furthermore, the trade-offs among sweeping rate, dynamic linewidth, and scanning bandwidth in our system have been observed. By properly adjusting the difference in optical wavelengths between sweeping and fixed wavelength lasers and using sub-THz photodiode, the generation of sub-THz chirped waveform with high tunability can be expected.

Acknowledgements

This project is sponsored by the National Science Council of Taiwan and Asian Office of Aerospace Research and Development (AOARD) under NSC100-2120-M-002-005 and AOARD-13-4088, respectively. The authors would also like to thank the helpful discussions with Prof. Andrew M. Weiner at Prude University